Hindawi
Advances in Materials Science and Engineering
Volume 2018, Article ID 2460403, 13 pages
https://doi.org/10.1155/2018/2460403

Research Article

A Mix Design Procedure for Alkali-Activated High-Calcium Fly Ash Concrete Cured at Ambient Temperature

Tanakorn Phoo-ngernkham[1], **Chattarika Phiangphimai**[1], **Nattapong Damrongwiriyanupap**[2], **Sakonwan Hanjitsuwan**[3], **Jaksada Thumrongvut**[1], **and Prinya Chindaprasirt**[4,5]

[1]*Department of Civil Engineering, Faculty of Engineering and Architecture, Rajamangala University of Technology Isan, Nakhon Ratchasima 30000, Thailand*
[2]*Civil Engineering Program, School of Engineering, University of Phayao, Phayao 56000, Thailand*
[3]*Program of Civil Technology, Faculty of Industrial Technology, Lampang Rajabhat University, Lampang 52100, Thailand*
[4]*Sustainable Infrastructure Research and Development Center, Department of Civil Engineering, Faculty of Engineering, Khon Kaen University, Khon Kaen 40002, Thailand*
[5]*Academy of Science, The Royal Society of Thailand, Dusit, Bangkok 10300, Thailand*

Correspondence should be addressed to Tanakorn Phoo-ngernkham; tanakorn.ph@rmuti.ac.th

Received 31 December 2017; Revised 3 March 2018; Accepted 25 March 2018; Published 15 April 2018

Academic Editor: Marino Lavorgna

This research focuses on developing a mix design methodology for alkali-activated high-calcium fly ash concrete (AAHFAC). High-calcium fly ash (FA) from the Mae Moh power plant in northern Thailand was used as a starting material. Sodium hydroxide and sodium silicate were used as alkaline activator solutions (AAS). Many parameters, namely, NaOH concentration, alkaline activator solution-to-fly ash (AAS/FA) ratio, and coarse aggregate size, were investigated. The 28-day compressive strength was tested to validate the mix design proposed. The mix design methodology of the proposed AAHFAC mixes was given step by step, and it was modified from ACI standards. Test results showed that the 28-day compressive strength of 15–35 MPa was obtained. After modifying mix design of the AAHFAC mixes by updating the AAS/FA ratio from laboratory experiments, it was found that they met the strength requirement.

1. Introduction

Recently, alkali-activated binders have been widely studied to be used as a substitute for Portland cement. This is because they show great promise as an environmentally friendly binder, have high strength, are stable at high temperatures, and have high durability which are similar to those of Portland cement [1, 2]. From the past, alkali-activated binders are certainly emerged as a novel construction material and have a huge potential to become a prominent construction product of good environmental sustainability [3]. Alkali-activated binders are normally obtained from amorphous aluminosilicate materials such as fly ash, calcined kaolin, or metakaolin activated with high alkali solutions [4–8]. The sodium aluminosilicate hydrate (N-A-S-H) gel is the main reaction product for the low-calcium system, while calcium silicate hydrate (C-S-H) and calcium aluminosilicate hydrate (C-A-S-H) gels coexisted with sodium aluminosilicate hydrate (N-A-S-H) gel are the main reaction products for the high-calcium system [7, 9]. In Thailand, high-calcium fly ash (FA) from the Mae Moh power plant in the north of Thailand is a widely used starting material for making alkali-activated binders. High CaO content from this FA is very attractive for making alkali-activated binders because it can enhance the strength development when cured at ambient temperature [10–15]. This is why alkali-activated binders are needed to be used in practical works.

Table 1: Chemical compositions of FA (by weight).

Materials	SiO_2	Al_2O_3	Fe_2O_3	CaO	MgO	K_2O	Na_2O	SO_3	LOI
FA	31.32	13.96	15.64	25.79	2.94	2.93	2.83	3.29	1.30

Table 2: Material properties of the AAHFAC ingredients.

Materials	Specific gravity	Fineness modulus	Absorption capacity (%)	Dry density (kg/m^3)
FA	2.65	—	—	—
RS	2.52	2.20	0.85	1585
7 mm·LS	2.64	6.04	1.55	1420
10 mm·LS	2.65	7.00	1.50	1405
16 mm·LS	2.67	7.09	1.00	1400

It is well known that alkali activator solution is one of the most important factors influencing the strength development of alkali-activated binders. From previous study on this area by Pimraksa et al. [16], they reported that sodium hydroxide and sodium silicate solutions were widely used as liquid activators because of availability and good mechanical properties. Panias et al. [17] claimed that sodium hydroxide solution is commonly used for the dissolution of Si^{4+} and Al^{3+} ions from FA to form aluminosilicate materials, whereas sodium silicate solution contains soluble silicate species and thus is used to promote the condensation process of alkali-activated binders [13]. Many researchers [6, 13, 18–20] reported that a combination of sodium silicate and sodium hydroxide solutions showed the best mechanical performance of alkali-activated binders.

To be useful in practice, a mix design methodology of alkali-activated binders has been studied. For example, Lloyd et al. [21] conducted a mix design methodology for alkali-activated low-calcium fly ash concrete. Ananda Kumar and Sankara Narayanan. [22] studied a design procedure for different grades of alkali-activated concrete by using Indian standards. In this method, fly ash content and activator solution-to-fly ash ratio were selected based on the strength requirement and by keeping the fine aggregate percentage as constant. Ferdous et al. [23] proposed a mix design for fly ash-based alkali-activated binders concrete by considering the concrete density variability, specific gravity of the materials, air content, workability, and the strength requirement. Also, Lahoti et al. [24] studied the mix design factor and strength prediction of metakaolin-based geopolymer, but it was just a study on the basic properties of the geopolymer made from metakaolin which were not applicable for other raw materials such as fly ash and slag. There were few research studies conducted by Anuradha et al. [22] and Ferdous et al. [23] that used the trial-and-error approach for considering a mix design of alkali-activated binders. However, mix design and proportion of containing binders of alkali-activated concrete seem to be complex because more variables are being involved in it. Therefore, there is no standard mix design method available for designing alkali-activated binders concrete to date. According to the recent study, Pavithra et al. [25] studied a mix design procedure for alkali-activated low-calcium FA concrete. It is shown that its strength follows a similar trend to that of Portland cement concrete as per ACI standards. However, this work still used the temperature curing for enhancing the strength development. From the literature review, there is no research investigated on a mix design methodology for alkali-activated high-calcium FA concrete. Therefore, in this research, we attempt to make a new mix design methodology for alkali-activated high-calcium FA concrete. Many parameters, namely, NaOH concentration, alkaline activator solution-to-binder ratio, and coarse aggregate size, have been investigated. Engineering properties, that is, setting time, compressive strength, flexural strength, modulus of elasticity, and Poisson's ratio, of the AAHFAC have been tested to understand behaviors for utilizing this material in the future. The step-by-step procedure of the mix design for alkali-activated high-calcium FA concrete will be explained in this paper. The outcome of this study would lay a foundation for the future use of alkali-activated high-calcium FA concrete for manufacturing this material in construction work.

2. Experimental Details

2.1. Materials. The precursor used in this study is fly ash (FA) from lignite coal combustion. The FA is the byproduct from the Mae Moh power plant in northern Thailand with a specific gravity of 2.65, a mean particle size of 15.6 μm, and a Blaine fineness of 4400 cm^2/g, respectively. Table 1 summarizes the chemical compositions of the FA used in the present experimental work. Note that the FA had a sum of $SiO_2 + Al_2O_3 + Fe_2O_3$ at 60.96% and CaO at 25.79%. Therefore, this FA was classified as class C FA as per ASTM C618 [26]. The fine aggregate is the local river sand (RS) with a specific gravity of 2.52 and a fineness modulus of 2.20, while coarse aggregates are the crushed lime stone (LS) with various different average sizes of 7, 10, and 16 mm, respectively. Material properties of alkali-activated high-calcium fly ash concrete (AAHFAC) ingredients are illustrated in Table 2.

Sodium hydroxide solution (NaOH) and sodium silicate solution (Na_2SiO_3) with 11.67% Na_2O, 28.66% SiO_2, and 59.67% H_2O were used as liquid activators. For example, for the preparation of 10 M·NaOH, sodium hydroxide pellets of 400 gram were dissolved by distilled water of 1 liter and then

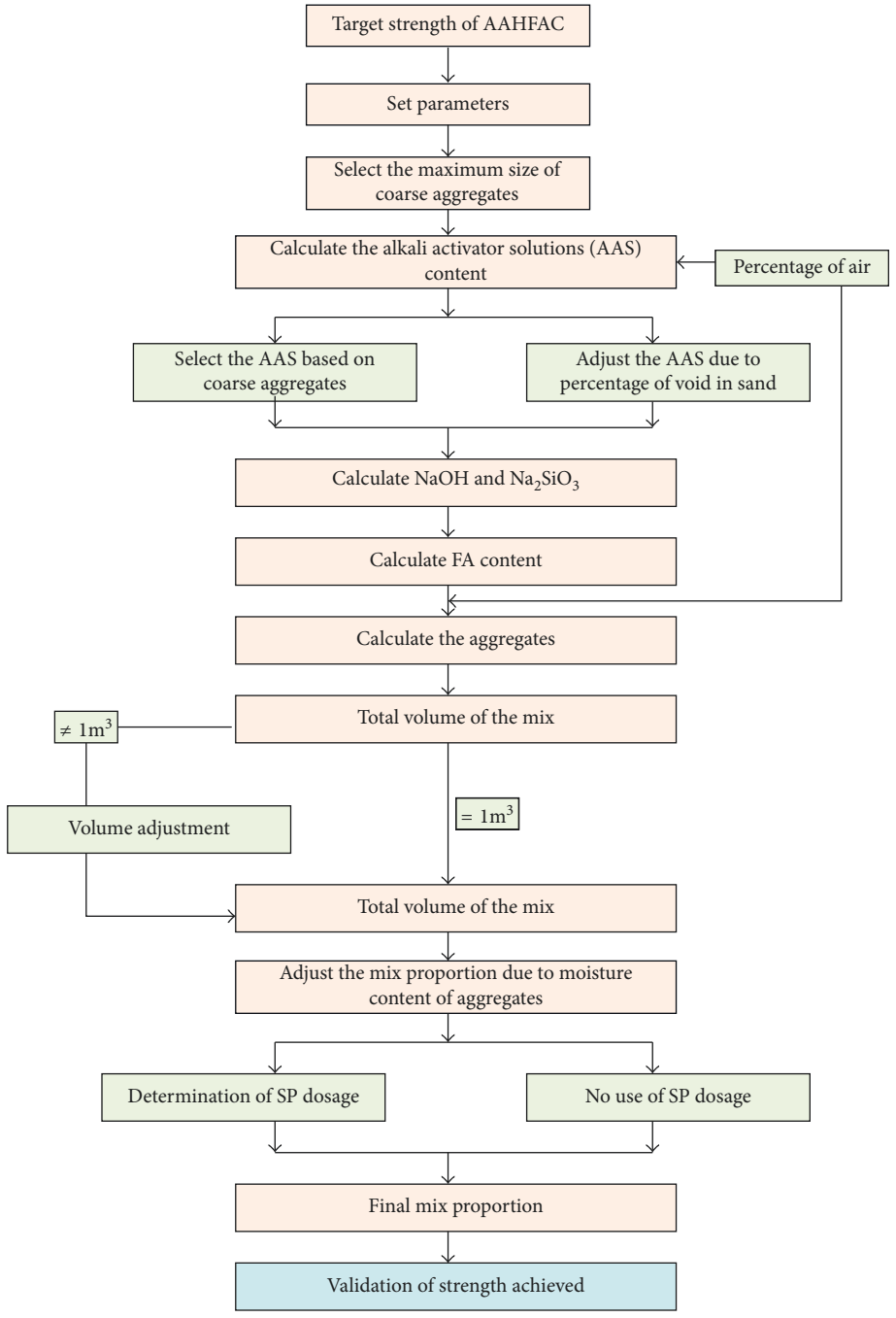

Figure 1: Flow chart for the mix design procedure.

allowed to cool down for 24 hours before use to avoid the uncontrolled acceleration of setting of alkali-activated binders [27–29].

2.2. Proposed Method for Designing Alkali-Activated High-Calcium Fly Ash Concrete. In this paper, we propose a novel mix design methodology for alkali-activated high-calcium fly ash concrete (AAHFAC) in a rational approach. It should be noted that the method is easy to use because it is based on the ACI 211.4R-93 [30] with some modification. The parametric studies are composed of different NaOH concentrations, alkaline activator solution- (AAS-) to-binder ratios, and coarse aggregate sizes. The flow chart for the mix design procedure in this study is illustrated in Figure 1. The step-by-step procedure is summarized as follows:

(1) Step 1: selection of the maximum size of the coarse aggregate

This step is to select the maximum sizes of coarse aggregates for mixing the AAHFAC. Three different sizes of coarse aggregates have been investigated, namely, 4.5–9.5 mm or average 7 mm, 9.5–12.5 mm or average 10 mm, and 12.5–20.0 mm or average 16 mm.

Table 3: Maximum water content and percentage of air per cubic meter of concrete [31].

Normal maximum size of the aggregate (mm)	Maximum water content (kg/m^3)	Percentage of void (%)
10	225	3.0
12.5	215	2.5
20	200	2.0

(2) Step 2: selection of the alkaline activator solution (AAS) content and air content

AAS content and air content were based on the maximum coarse aggregate size as per ACI standards. Maximum AAS and percentage of air per cubic meter of concrete in this study were selected by using the slump condition of around 20 mm as per ACI standards. This condition is summarized in Table 3.

(3) Step 3: adjustment of the alkaline activator solution (AAS) content due to percentage of void in the fine aggregate

As per ACI 211.4R-93 [30], a mixture of concrete has been recommended to use the fine aggregate with fineness modulus values from 2.4 to 3.2. However, particle shape and surface texture of the fine aggregate have an effect on its voids content; therefore, mixing water requirements may be different from the values given. As mentioned, the values for the required mixing water given are applicable when the fine aggregate is used that has a void content of 35%. If not, an adjustment of water content must be added into the required water content. Therefore, this study will calculate the AAS content due to percentage of void in the fine aggregate in a similar way to Portland cement concrete. This adjustment can be calculated using the following equation:

$$\mathrm{AAS}_{\mathrm{adjustment}} = \left|\left\{\left[1 - \left(\frac{\rho_{\mathrm{RS}}}{S_{\mathrm{G}}\rho_{\mathrm{w}}}\right)\right] \times 100\right\} - 35\right| \times 4.75, \quad (1)$$

where $\mathrm{AAS}_{\mathrm{adjustment}}$ is an adjustment of the AAS content (kg/m^3), ρ_{RS} is the density of the fine aggregate in SSD condition (kg/m^3), S_{G} is the specific gravity of the fine aggregate, and ρ_{w} is the density of water (kg/m^3).

(4) Step 4: selection of alkaline activator solution-to-fly ash (AAS/FA) ratio

This research attempts in adopting the standard AAS-to-FA ratio curve of the AAHFAC before use. The minimum compressive strength could be determined from the relationship between 28-day compressive strength and AAS-to-FA ratio. Only the compressive strength of AAHFAC was considered as it is the requirement as per ACI 211.4R-93 [30].

(5) Step 5: calculation of binder content

The weight of the binder required per cubic meter of the AAHFAC could be determined by dividing the values of mixing the AAS content after an adjustment of the AAS content due to percentage of void in the fine aggregate.

(6) Step 6: calculation of individual mass of AAS content (NaOH and Na_2SiO_3 solutions)

Table 4: Density of NaOH solution with different concentrations.

NaOH (molar)	5 M	10 M	15 M
Density (kg/m^3)	1200	1413	1430

From the literature, NaOH and Na_2SiO_3 were found to be the commonly used alkali activators [21]. In this study, NaOH and Na_2SiO_3 have been selected as alkaline activator solutions. According to Table 4, the density of NaOH with different concentrations has been used for calculating the volume of AAS as per the volume method. The individual mass of alkaline activator solutions content could be calculated using the following equation:

$$\mathrm{Na_2SiO_3} = \frac{\mathrm{AAS}}{\left[1 + \left(1/\left(\mathrm{Na_2SiO_3}/\mathrm{NaOH}\right)\right)\right]},$$
$$\mathrm{NaOH} = \mathrm{AAS} - \frac{\mathrm{AAS}}{\left[1 + \left(1/\left(\mathrm{Na_2SiO_3}/\mathrm{NaOH}\right)\right)\right]}. \quad (2)$$

(7) Step 7: calculation of fine and coarse aggregates

The mass of fine and coarse aggregates content is determined as per the absolute volume method. Let the percentage of the fine aggregate in the total aggregate be 30% and that of the coarse aggregate be 70%. Fine and coarse aggregates content are determined using the following equation:

$$M_{\mathrm{RS}} = 0.3S_{\mathrm{G(RS)}}\left[1 - V_{\mathrm{FA}} - V_{\mathrm{NaOH}} - V_{\mathrm{Na_2SiO_3}} - V_{\mathrm{air}}\right] \times 1000,$$
$$M_{\mathrm{LS}} = 0.7S_{\mathrm{G(LS)}}\left[1 - V_{\mathrm{FA}} - V_{\mathrm{NaOH}} - V_{\mathrm{Na_2SiO_3}} - V_{\mathrm{air}}\right] \times 1000, \quad (3)$$

where M_{RS} is the mass of the fine aggregate (kg), M_{LS} is the mass of the coarse aggregate (kg), $S_{\mathrm{G(RS)}}$ is the specific gravity of the fine aggregate, $S_{\mathrm{G(LS)}}$ is the specific gravity of the coarse aggregate, V_{FA} is the volume of high-calcium fly ash, V_{NaOH} is the volume of NaOH, $V_{\mathrm{Na_2SiO_3}}$ is the volume of Na_2SiO_3, and V_{air} is the volume of entrapped air.

(8) Step 8: calculation of superplasticizer dosage

The AAS has the higher viscosity than tap water when used for making the AAHFAC. Hardjito et al. [32] reported that the dosage of the superplasticizer was effective for the range between 0.8 and 2% of binder content to improve the workability of alkali-activated binder concrete. Pavithra et al. [25] also claimed that the use of superplasticizer dosage was found to have impact on behavior of fresh alkali-activated binder concrete; however, it had a little effect on strength and other properties. Therefore, to improve the workability of the AAHFAC, a small amount of the superplasticizer was incorporated in the mixture.

(9) Step 9: validation of strength attained with the proposed mix design

The 28-day compressive strength obtained from testing will be verified with the target strength.

(10) Step 10: recalculation of Step 4 by the strength obtained from Step 9

Table 5: Mix proportion used in this study based on the mix design procedure.

Mix	Symbol	FA (kg/m^3)	NaOH (kg/m^3)		Na_2SiO_3 (kg/m^3)	Aggregates (kg/m^3)				SP (kg/m^3)
			10 M	15 M		7 mm·LS	10 mm·LS	16 mm·LS	RS	
1	0.45AAS10M7mmLS	523	118	—	118	1124	—	—	459	5.2
2	0.45AAS10M10mmLS	500	113	—	113	—	1166	—	475	5.0
3	0.45AAS10M16mmLS	478	108	—	108	—	—	1211	490	4.8
4	0.50AAS10M7mmLS	470	118	—	118	1161	—	—	474	4.7
5	0.50AAS10M10mmLS	450	113	—	113	—	1201	—	489	4.5
6	0.50AAS10M16mmLS	430	108	—	108	—	—	1245	504	4.3
7	0.55AAS10M7mmLS	428	118	—	118	1191	—	—	487	4.3
8	0.55AAS10M10mmLS	409	113	—	113	—	1231	—	501	4.1
9	0.55AAS10M16mmLS	391	108	—	108	—	—	1273	515	3.9
10	0.60AAS10M7mmLS	392	118	—	118	1216	—	—	497	3.9
11	0.60AAS10M10mmLS	375	113	—	113	—	1255	—	511	3.8
12	0.60AAS10M16mmLS	359	108	—	108	—	—	1296	525	3.6
13	0.45AAS15M7mmLS	523	—	118	118	1126	—	—	460	5.2
14	0.45AAS150M10mmLS	500	—	113	113	—	1168	—	475	5.0
15	0.45AAS15M16mmLS	478	—	108	108	—	—	1212	491	4.8
16	0.50AAS15M7mmLS	470	—	118	118	1163	—	—	475	4.7
17	0.50AAS15M10mmLS	450	—	113	113	—	1203	—	490	4.5
18	0.50AAS15M16mmLS	430	—	108	108	—	—	1246	505	4.3
19	0.55AASB15M7mmLS	428	—	118	118	1193	—	—	487	4.3
20	0.55AAS15M10mmLS	409	—	113	113	—	1232	—	502	4.1
21	0.55AAS15M16mmLS	391	—	108	108	—	—	1274	516	3.9
22	0.60AASB150M7mmLS	392	—	118	118	1218	—	—	498	3.9
23	0.60AAS15M10mmLS	375	—	113	113	—	1257	—	512	3.8
24	0.60AAS15M16mmLS	359	—	108	108	—	—	1298	525	3.6

After the 28-day compressive strength has been obtained from testing, all strengths will be recalculated in Step 4 for determining the strength requirement of the AAHFAC with various AAS-to-FA ratios.

(11) Step 11: validation of strength achieved

Compressive strength tests will be conducted in the laboratory using the mix design proposed above. When the designed mix satisfies the strength requirement, the final development of the AAHFAC can be made by employing the above design steps.

2.3. Manufacturing and Testing of the AAHFAC. The laboratory experiments have been conducted to validate the proposed mix design. Based on the AAHFAC trial mix, high-calcium fly ash (FA) from the Mae Moh power plant in northern Thailand is used as a starting material for making the AAHFAC. Constant $NaOH/Na_2SiO_3$ ratio is fixed at 1.0 in all mixes. The AAHFAC has been manufactured with different NaOH concentrations of 10 M and 15 M. Both fine and coarse aggregates in saturated surface dry (SSD) condition have been used for making the AAHFAC. Crushed lime stone with different average sizes of 7, 10, and 16 mm, respectively, is investigated. In this present work, mix design of the AAHFAC with slump at around 17.5–22.5 mm or average 20 mm has been controlled in order to ensure the workability of the AAHFAC.

For the mixing of the AAHFAC, fine and coarse aggregates were mixed together first for 60 s. After that, NaOH solution was added, and then, they were mixed again for 30 s. After 30 s, FA was added, and then, the mixture was mixed for 60 s. Afterward, Na_2SiO_3 solution and superplasticizer were added into the mixture, and the mixture was mixed again for a further 60 s until becoming homogeneous. The mix proportions of the AAHFAC are illustrated in Table 5.

After mixing, the workability of the AAHFAC was tested using the slump cone test as per ASTM C143 [33] as shown in Figure 2. Setting time of the AAHFAC was evaluated using the method of penetration resistance as per ASTM C403/C403M-16 [34]. After that, a fresh AAHFAC was placed into a cylinder mold with 100 mm diameter and 200 mm height to measure the compressive strength, modulus of elasticity, and Poisson's ratio. Tests for the determination of the static chord modulus of elasticity and Poisson's ratio of the samples have been carried out as per ASTM C469 [35]. The 75 × 75 × 300 mm3 long beam was used to measure the flexural strength of the AAHFAC, and the flexural strength was calculated as per ASTM C78 [36]. The test setup for the compressive strength, flexural strength, modulus of elasticity, and Poisson's ratio of the AAHFAC is illustrated in Figures 3 and 4. After curing, the AAHFAC samples were demolded with the aid of slight tapping at the side of the mold at the age of 1 day and immediately wrapped with vinyl sheet to protect moisture loss and kept at the ambient room temperature. All samples of the compressive strength, flexural strength, modulus of elasticity, and Poisson's ratio were tested at the age of 28 days of curing of the AAHFAC. Five identical samples were tested for each mix, and the average value was used as the test result.

(a) (b)

Figure 2: Fresh AAHFAC (a) and slump test of the AAHFAC (b).

Figure 3: Test setup for compressive strength, modulus of elasticity, and Poisson's ratio.

Figure 4: Test setup for flexural strength.

3. Experimental Results and Discussion

Figures 5–10 show the test results of fresh AAHFAC and mechanical properties of the AAHFAC. According to Figure 5, the slump values are between 18 and 22 mm; therefore, mix design of the AAHFAC from Table 5 is in line with the slump value at around 17.5–22.5 mm. As mentioned, the AAS and air contents based on the maximum size of the aggregate as per the ACI standard could be taken for this study. The final setting time of the AAHFAC tends to obviously increase with the increase of AAS/FA ratio and NaOH concentration as illustrated in Figure 6. This result conforms to the previous studies [37, 38] that an increase of fluid medium content resulted in less particle interaction and increased the workability of the mixture. Hanjitsuwan et al. [39] and Rattanasak and Chindaprasirt [40] also explained that NaOH concentration is a main reason for leaching out of Si^{4+} and Al^{3+} ions; therefore, the time of setting tends to increase. However, different sizes of the coarse aggregate are marginal changed in the setting time of the AAHFAC.

Test results of the compressive strength, modulus of elasticity, and Poisson's ratio have been shown in Figures 7 and 8. It is found that the compressive and flexural strengths tend to increase with the increase of AAS/FA ratio and NaOH concentration; however, they are decreased with increasing coarse aggregate sizes. Sinsiri et al. [38] claimed that the excess OH^- concentration in the mixture at high AAS/FA ratio causes the decrease of strength development of the AAHFAC similar to that in case of increasing water-to-cement ratios for Portland cement concrete. Also, the excess liquid solution could disrupt the polymerization process [37]. For the effect of NaOH concentration, it is found that the increase in the leaching out of Si^{4+} and Al^{3+} ions from FA particles at high NaOH concentration could improve the N-A-S-H gel, and thus, it gives high strength development of the AAHFAC [40]. Also, CaO oxide could react with silica and alumina from FA to form C-(A)-S-H gel which coexisted with N-A-S-H gel [11, 12, 14, 15, 20], resulting in an enhancement of strength. The short setting time of less than 60 minutes at ambient temperature with relatively high 28-day compressive strengths of 16.0–36.0 MPa indicated the role of calcium in the system. Therefore, the AAHFAC could be used as an alternative repair material as reported by several publications [13, 14, 20, 29, 41–43]. There are many reasons such as high compressive strength [44], negligible drying shrinkage [45], low creep [46], good bond with reinforcing steel [47, 48], good resistance to acid and sulfate [3, 27], fire resistance [49], and excellent bond with old concrete [14, 20, 28]. For the effect of coarse aggregate size, the strength development tends to decrease with the increase of coarse aggregate size. Generally,

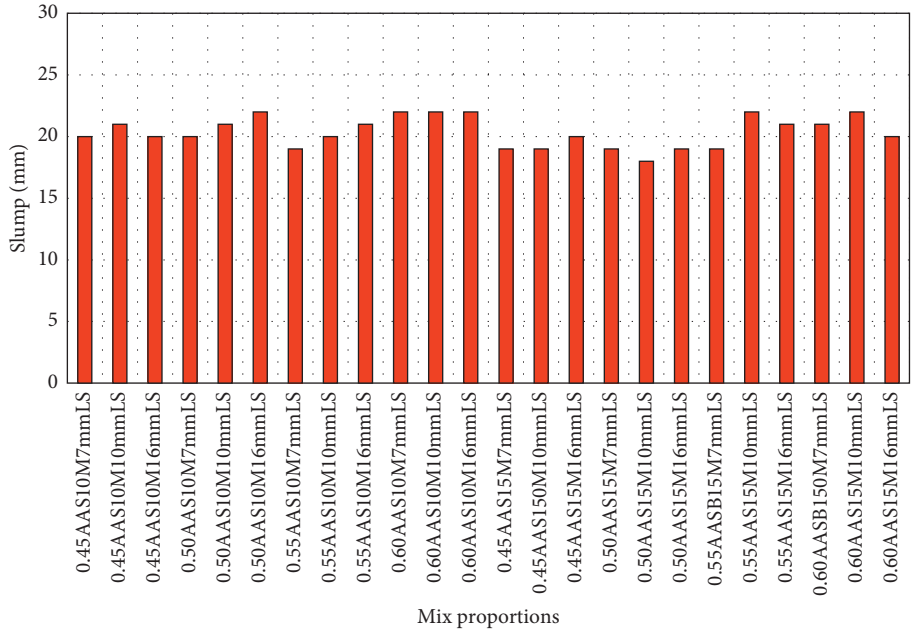

Figure 5: Slump of the AAHFAC

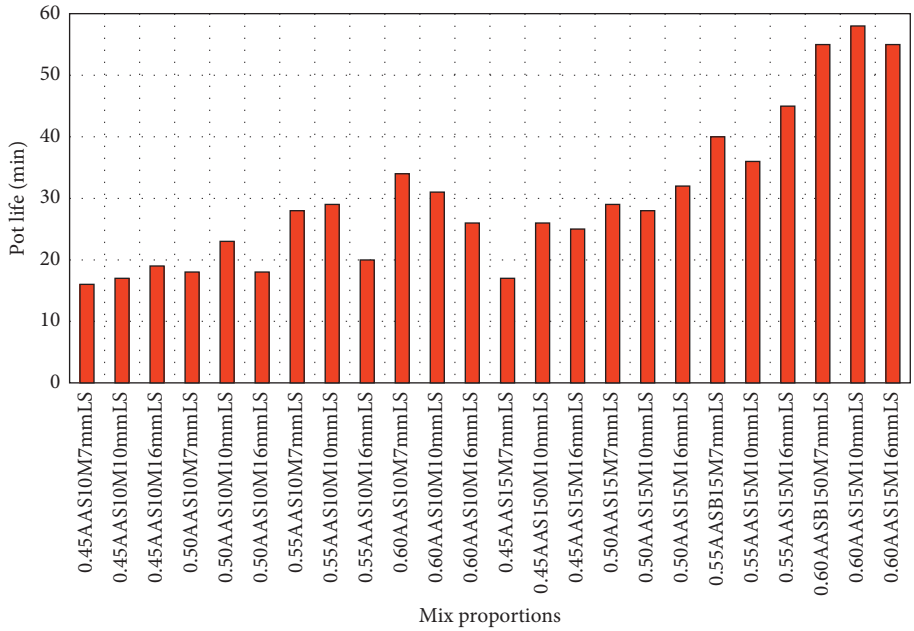

Figure 6: Pot life of the AAHFAC.

the binder within the AAHFAC is an important factor on the strength development of the matrix. This agrees with the findings of Pavithra et al. [25] that the increase in total aggregate corresponding to the decrease of paste has an adverse effect on the strength development of low-calcium fly ash geopolymer concrete.

The experimental results obtained for the modulus of elasticity and Poisson's ratio of the AAHFAC mixes show an overall increase with the increase of compressive strength as shown in Figures 9 and 10; however, the coarse aggregate size influenced the modulus of elasticity and Poisson's ratio. Normally, it is well known that the values of modulus of elasticity and Poisson's ratio of concrete depend on the stiffness of paste and aggregates [50]. The modulus of elasticity obtained from this study agrees with Nath and Sarker [51] that the modulus of elasticity of geopolymer concrete with 28-day compressive strength of 25–45 MPa was between 17.4 and 24.6 GPa, while the modulus of elasticity of Portland cement concrete was between 25 and 35 GPa [51, 52]. According to Figure 10, Poisson's ratio for

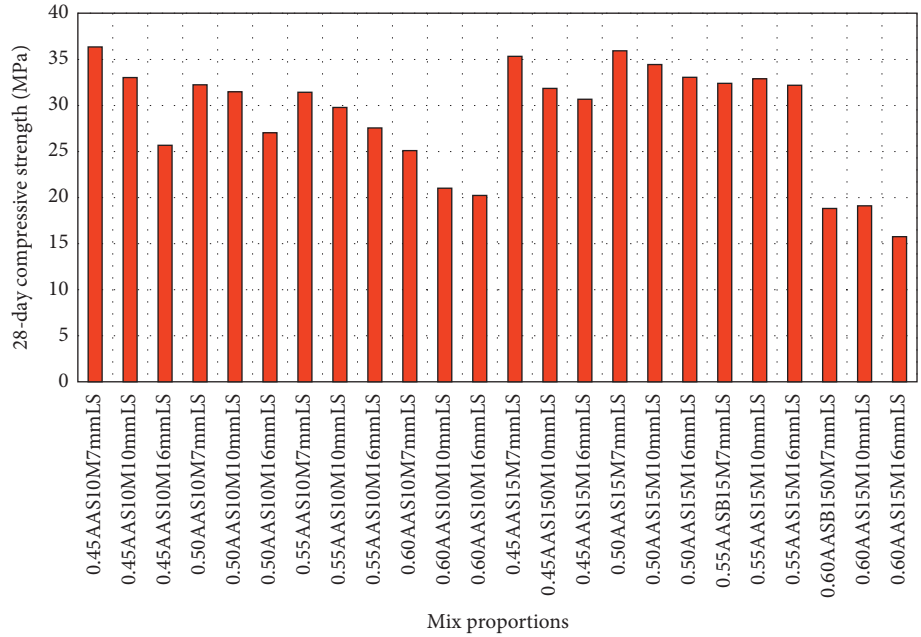

Figure 7: 28-day compressive strength of the AAHFAC.

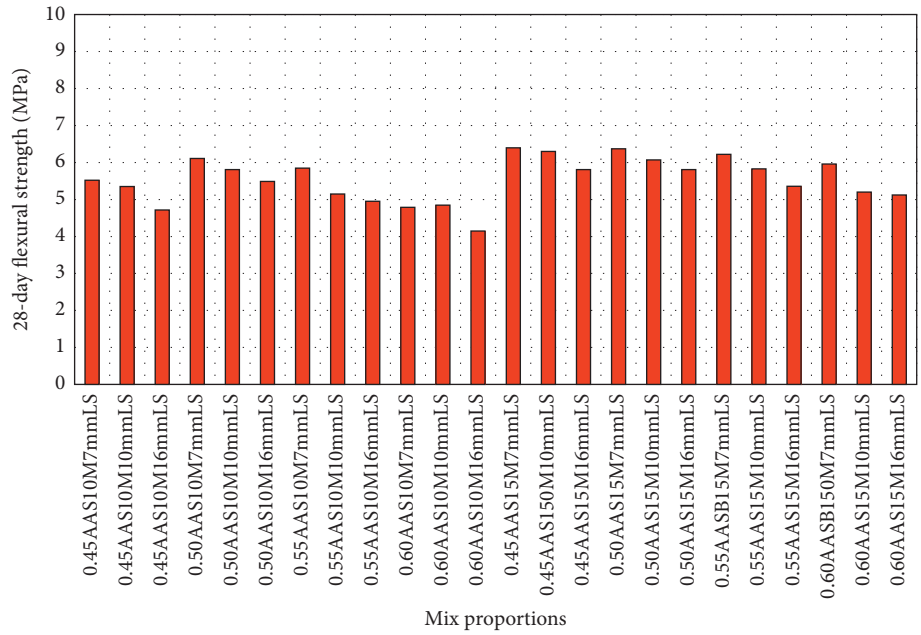

Figure 8: 28-day flexural strength of the AAHFAC.

all of the AAHFAC mixes is between 0.21 and 0.31. They show values slightly higher than the values assigned for normal strength of Portland cement concrete which are between 0.11 and 0.21 [50]. The high Poisson's ratios were associated with the mixes with large aggregates of 16 mm. For the mixes with smaller aggregates of 7 and 11 mm, Poisson's ratios are between 0.21 and 0.27 similar to the previously reported values of inorganic polymer concrete between 0.23 and 0.26 and also in the same range as those of high strength concrete between 0.20 and 0.25 [50].

4. Verification of the Mix Design Methodology Using Laboratory Experiments

To develop the mix design methodology of the AAHFAC, some parameters from laboratory experiments should be updated before use. In order to support the basic principles of mix design, the relationship between 28-day compressive strength and AAS/FA ratio from laboratory experiments has been produced as shown in Figure 11. The AAS/FA ratio curve can be determined for the minimum 28-day

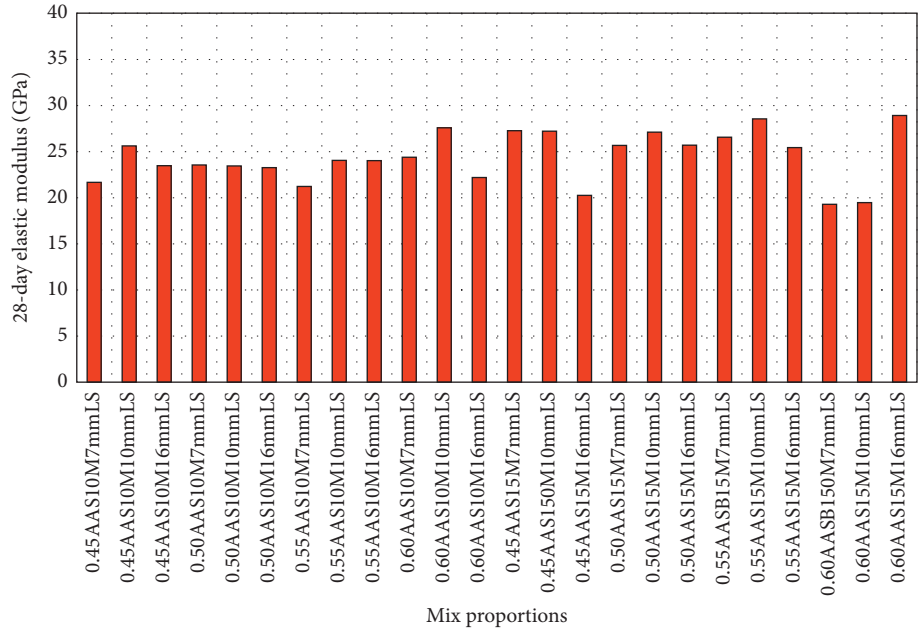

Figure 9: 28-day elastic modulus of the AAHFAC.

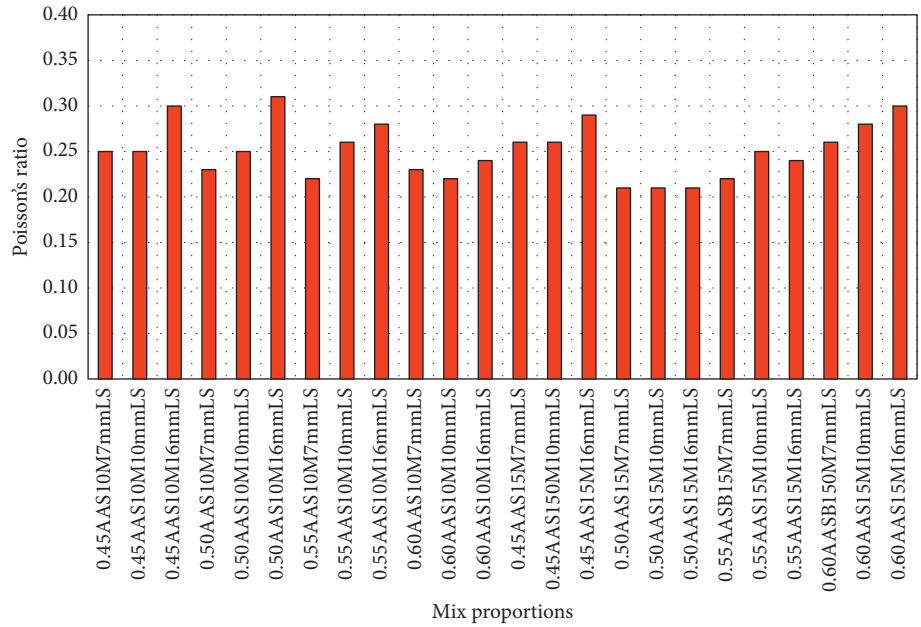

Figure 10: 28-day Poisson's ratio of the AAHFAC.

compressive strength of the AAHFAC similar to that of the water-to-cement ratio curve of Portland cement concrete.

According to Table 5 and Figures 5–10, the 24 different mixes of the AAHFAC were conducted to develop the mix design methodology. The 28-day compressive strength of the AAHFAC cured at ambient temperature ranging from 15 to 35 MPa was obtained by using the proposed mix design methodology. All obtained compressive strengths of the AAHFAC mixes can be separated into 5 strength requirements, namely, 15, 20, 25, 30, and 35 MPa, respectively. These obtained strength requirements of the AAHFAC will be used to recalculate in Step 4 for determining the strength requirement of the AAHFAC with various AAS/FA ratios (Figure 11).

In order to verify the mix design procedure, an example design of the AAHFAC mix with the target 28-day compressive strength of 30 MPa has been considered. The parameters are NaOH concentration of 10 M, maximum aggregate size of 10 mm, and Na_2SiO_3/NaOH ratio of 1.0. Material properties of the AAHFAC ingredients are

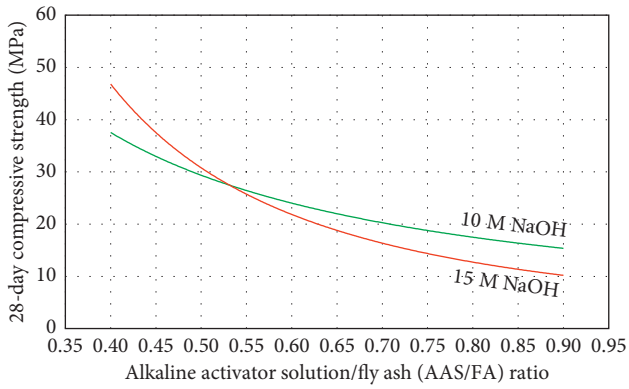

Figure 11: Twenty-eight-day compressive strength versus the AAS/FA ratio curve.

illustrated in Table 2. The step-by-step procedure of the mix design is explained as follows:

Step 1: selection of the maximum coarse aggregate size

This mix design of the AAHFAC has been selected the maximum coarse aggregate size of 10 mm for mixing the AAHFAC.

Step 2: selection of AAS and air contents

AAS and air contents are based on the maximum size of the coarse aggregate; therefore, AAS content of 225 kg/m^3 and air content of 3.0% have been used as given in Table 3.

Step 3: adjustment of AAS content due to percentage of void in the fine aggregate

The fine aggregate used in this example has a void of 37%; therefore, the value of adjustment could be calculated as follows:

$$\mathrm{AAS}_{\mathrm{adjustment}} = \left|\left\{\left[1-\left(\frac{1585}{2.52*1000}\right)\right]\times 100\right\}-35\right| \times 4.75 = 10\ \mathrm{kg/m^3}. \quad (4)$$

Therefore, the AAS content after an adjustment of AAS content due to percentage of void in the fine aggregate is 235 kg/m^3.

Step 4: selection of AAS/FA ratio

From Figure 11, for the minimum 28-day compressive strength of 30 MPa, it is found that the AAS/FA ratio of 0.50 is obtained when 10 M·NaOH was used as alkaline activator solution.

Step 5: calculation of binder content

$$\text{FA content} = \frac{\text{AAS content}}{\text{AAS/FA ratio}} = \frac{235}{0.50} = 470\ \mathrm{kg/m^3}. \quad (5)$$

Step 6: calculation of NaOH and Na_2SiO_3 content

The individual mass of NaOH and Na_2SiO_3 content could be calculated as follows:

$$\begin{aligned}\mathrm{Na_2SiO_3} &= \frac{\mathrm{AAS}}{\left[1+\left(1/\left(\mathrm{Na_2SiO_3/NaOH}\right)\right)\right]} \\ &= \frac{235}{[1+(1/1)]} = 117.50\ \mathrm{kg/m^3}, \\ \mathrm{NaOH} &= \mathrm{AAS}-\frac{\mathrm{AAS}}{\left[1+\left(1/\left(\mathrm{Na_2SiO_3/NaOH}\right)\right)\right]} \\ &= 117.50-\frac{235}{[1+(1/1)]} = 117.50\ \mathrm{kg/m^3}.\end{aligned} \quad (6)$$

Step 7: calculation of fine and coarse aggregates

$$\begin{aligned}M_{\mathrm{RS}} &= 0.3(2.52)\left[1-\frac{470}{2.65\times 1000}-\frac{117.5}{1413}-\frac{117.5}{1485}-\frac{3}{100}\right] \\ &\quad \times 1000 = 477\ \mathrm{kg/m^3}, \\ M_{\mathrm{LS}} &= 0.7(2.64)\left[1-\frac{470}{2.65\times 1000}-\frac{117.5}{1413}-\frac{117.5}{1485}-\frac{3}{100}\right] \\ &\quad \times 1000 = 1164\ \mathrm{kg/m^3}.\end{aligned} \quad (7)$$

Step 8: calculation of superplasticizer dosage

$$\text{SP dosage} = \left(\frac{1}{100}\right)\times 470 = 4.7\ \mathrm{kg/m^3}. \quad (8)$$

Step 9: summarization of mix design

Based on the mix design methodology of the AAHFAC mix, mix proportions of ingredients are concluded as follows:

$$\begin{aligned}\mathrm{FA} &= 470\ \mathrm{kg/m^3}, \\ \mathrm{RS} &= 477\ \mathrm{kg/m^3}, \\ \mathrm{LS} &= 1164\ \mathrm{kg/m^3}, \\ \mathrm{NaOH} &= 117.5\ \mathrm{kg/m^3}, \\ \mathrm{Na_2SiO_3} &= 117.5\ \mathrm{kg/m^3}, \\ \mathrm{SP} &= 4.7\ \mathrm{kg/m^3}.\end{aligned} \quad (9)$$

Step 10: validation of strength achieved

After following the mix design of the AAHFAC mix, the AAHFAC samples were tested for compressive strength on cylinder molds with 100 mm diameter and 200 mm height. After testing, it is found that the 28-day compressive strength of the AAHFAC is 31.15 MPa. Therefore, the mix design of the AAHFAC above meets the strength requirement.

5. Conclusion

In this study, the novel mix design methodology for alkali-activated high-calcium fly ash concrete (AAHFAC) cured at ambient temperature in a rational way was proposed. From

the review of mix design of alkali-activated binders concrete, there is no standard mix design method available for designing the AAHFAC. Some works have been investigated in this area in an attempt to develop mix design methodology for alkali-activated low-calcium fly ash. However, it still used the temperature curing for enhancing the strength development of alkali-activated low-calcium fly ash, but this is limited for construction work. To be useful in practice, alkali-activated binders concrete cured at ambient temperature has been used to solve this problem. In this study, a new mix design methodology for AAHFAC was modified from ACI standards. The step-by-step procedure of the mix design for the AAHFAC mixes has been explained in the earlier section. From laboratory experiments, the 28-day compressive strength of the AAHFAC cured at ambient temperature ranging from 15 to 35 MPa was obtained. After compressive strength was obtained, the alkaline activator solution-to-binder ratios were used to modify the mix design of the AAHFAC. Using the modified mix design of the AAHFAC mix, it is found that the proposed mix design of the AAHFAC in this study meets the strength requirement. This mix design would lay a foundation for the future use of AAHFAC in construction industry.

Conflicts of Interest

The authors declare that there are no conflicts of interest.

Acknowledgments

This work was financially supported by the TRF New Research Scholar Grant no. MRG6080174 and the Thailand Research Fund (TRF) under the TRF Distinguished Research Professor Grant no. DPG6180002. The part of the present work was also supported by the European Commission Research Executive Agency via the Marie Skłodowska-Curie Research and Innovation Staff Exchange Project (689857-PRIGeoC-RISE-2015) and the Industry Academia Partnership Programme-2 (IAPP1617\16) "Development of Sustainable Geopolymer Concrete." The authors also would like to acknowledge the support of the Department of Civil Engineering, Faculty of Engineering and Architecture, Rajamangala University of Technology Isan, Thailand.

References

[1] F. Pacheco-Torgal, Z. Abdollahnejad, S. Miraldo, S. Baklouti, and Y. Ding, "An overview on the potential of geopolymers for concrete infrastructure rehabilitation," *Construction and Building Materials*, vol. 36, pp. 1053–1058, 2012.

[2] F. Xu, X. Deng, C. Peng, J. Zhu, and J. P. Chen, "Mix design and flexural toughness of PVA fiber reinforced fly ash-geopolymer composites," *Construction and Building Materials*, vol. 150, pp. 179–189, 2017.

[3] P. Chindaprasirt, P. Paisitsrisawat, and U. Rattanasak, "Strength and resistance to sulfate and sulfuric acid of ground fluidized bed combustion fly ash–silica fume alkali-activated composite," *Advanced Powder Technology*, vol. 25, no. 3, pp. 1087–1093, 2014.

[4] M. Albitar, P. Visintin, M. S. Mohamed Ali, and M. Drechsler, "Assessing behaviour of fresh and hardened geopolymer concrete mixed with class-F fly ash," *KSCE Journal of Civil Engineering*, vol. 19, pp. 1445–1455, 2015.

[5] Y. Jun and J. E. Oh, "Microstructural characterization of alkali-activation of six Korean class F fly ashes with different geopolymeric reactivity and their zeolitic precursors with various mixture designs," *KSCE Journal of Civil Engineering*, vol. 19, no. 6, pp. 1775–1786, 2015.

[6] S. Kumar, R. Kumar, and S. P. Mehrotra, "Influence of granulated blast furnace slag on the reaction, structure and properties of fly ash based geopolymer," *Journal of Materials Science*, vol. 45, no. 3, pp. 607–615, 2010.

[7] C. Li, H. Sun, and L. Li, "A review: the comparison between alkali-activated slag (Si + Ca) and metakaolin (Si + Al) cements," *Cement and Concrete Research*, vol. 40, no. 9, pp. 1341–1349, 2010.

[8] D. Ravikumar, S. Peethamparan, and N. Neithalath, "Structure and strength of NaOH activated concretes containing fly ash or GGBFS as the sole binder," *Cement and Concrete Composites*, vol. 32, no. 6, pp. 399–410, 2010.

[9] A. Palomo, M. W. Grutzeck, and M. T. Blanco, "Alkali-activated fly ashes: a cement for the future," *Cement and Concrete Research*, vol. 29, no. 8, pp. 1323–1329, 1999.

[10] T. Phoo-ngernkham, P. Chindaprasirt, V. Sata, S. Hanjitsuwan, and S. Hatanaka, "The effect of adding nano-SiO_2 and nano-Al_2O_3 on properties of high calcium fly ash geopolymer cured at ambient temperature," *Materials & Design*, vol. 55, pp. 58–65, 2014.

[11] T. Phoo-ngernkham, P. Chindaprasirt, V. Sata, S. Pangdaeng, and T. Sinsiri, "Properties of high calcium fly ash geopolymer pastes containing Portland cement as additive," *International Journal of Minerals, metallurgy and Materials*, vol. 20, no. 2, pp. 214–220, 2013.

[12] T. Phoo-ngernkham, P. Chindaprasirt, V. Sata, and T. Sinsiri, "High calcium fly ash geopolymer containing diatomite as additive," *Indian Journal of Engineering & Materials Sciences*, vol. 20, no. 2, pp. 214–220, 2013.

[13] T. Phoo-ngernkham, A. Maegawa, N. Mishima, S. Hatanaka, and P. Chindaprasirt, "Effects of sodium hydroxide and sodium silicate solutions on compressive and shear bond strengths of FA–GBFS geopolymer," *Construction and Building Materials*, vol. 91, pp. 1–8, 2015.

[14] T. Phoo-ngernkham, V. Sata, S. Hanjitsuwan, C. Ridtirud, S. Hatanaka, and P. Chindaprasirt, "High calcium fly ash geopolymer mortar containing Portland cement for use as repair material," *Construction and Building Materials*, vol. 98, pp. 482–488, 2015.

[15] T. Phoo-ngernkham, V. Sata, S. Hanjitsuwan, C. Ridtirud, S. Hatanaka, and P. Chindaprasirt, "Compressive strength, bending and fracture characteristics of high calcium fly ash geopolymer mortar containing Portland cement cured at ambient temperature," *Arabian Journal for Science and Engineering*, vol. 41, no. 4, pp. 1263–1271, 2016.

[16] K. Pimraksa, P. Chindaprasirt, A. Rungchet, K. Sagoe-Crentsil, and T. Sato, "Lightweight geopolymer made of highly porous siliceous materials with various Na_2O/Al_2O_3 and SiO_2/Al_2O_3 ratios," *Materials Science and Engineering A*, vol. 528, no. 21, pp. 6616–6623, 2011.

[17] D. Panias, I. P. Giannopoulou, and T. Perraki, "Effect of synthesis parameters on the mechanical properties of fly ash-based geopolymers," *Colloids and Surfaces A: Physicochemical and Engineering Aspects*, vol. 301, no. 1–3, pp. 246–254, 2007.

[18] A. M. Rashad, "Properties of alkali-activated fly ash concrete blended with slag," *Iranian Journal of Materials Science and Engineering*, vol. 10, no. 1, pp. 57–64, 2013.

[19] D. Ravikumar and N. Neithalath, "Effects of activator characteristics on the reaction product formation in slag binders activated using alkali silicate powder and NaOH," *Cement and Concrete Composites*, vol. 34, no. 7, pp. 809–818, 2012.

[20] T. Phoo-ngernkham, S. Hanjitsuwan, N. Damrongwiriyanupap, and P. Chindaprasirt, "Effect of sodium hydroxide and sodium silicate solutions on strengths of alkali activated high calcium fly ash containing Portland cement," *KSCE Journal of Civil Engineering*, vol. 21, no. 6, pp. 2202–2210, 2017.

[21] R. R. Lloyd, J. L. Provis, and J. S. J. van Deventer, "Pore solution composition and alkali diffusion in inorganic polymer cement," *Cement and Concrete Research*, vol. 40, no. 9, pp. 1386–1392, 2010.

[22] S. Ananda Kumar and T. S. N. Sankara Narayanan, "Thermal properties of siliconized epoxy interpenetrating coatings," *Progress in Organic Coatings*, vol. 45, no. 4, pp. 323–330, 2002.

[23] W. Ferdous, A. Manalo, A. Khennane, and O. Kayali, "Geopolymer concrete-filled pultruded composite beams–concrete mix design and application," *Cement and Concrete Composites*, vol. 58, pp. 1–13, 2015.

[24] M. Lahoti, P. Narang, K. H. Tan, and E. H. Yang, "Mix design factors and strength prediction of metakaolin-based geopolymer," *Ceramics International*, vol. 43, no. 14, pp. 11433–11441, 2017.

[25] P. Pavithra, M. Srinivasula Reddy, P. Dinakar, B. Hanumantha Rao, B. K. Satpathy, and A. N. Mohanty, "A mix design procedure for geopolymer concrete with fly ash," *Journal of Cleaner Production*, vol. 133, pp. 117–125, 2016.

[26] ASTM C618-15, "Standard specification for coal fly ash and raw or calcined natural pozzolan for use in concrete," in *Annual Book of ASTM Standard*ASTM International, West Conshohocken, PA, USA, 2015.

[27] S. Hanjitsuwan, T. Phoo-ngernkham, L. Y. Li, N. Damrongwiriyanupap, and P. Chindaprasirt, "Strength development and durability of alkali-activated fly ash mortar with calcium carbide residue as additive," *Construction and Building Materials*, vol. 162, pp. 714–723, 2018.

[28] T. Phoo-ngernkham, S. Hanjitsuwan, L. Y. Li, N. Damrongwiriyanupap, and P. Chindaprasirt, "Adhesion characterization of Portland cement concrete and alkali-activated binders under different types of calcium promoters," *Advances in Cement Research*, pp. 1–11, 2018.

[29] T. Phoo-ngernkham, S. Hanjitsuwan, C. Suksiripattanapong, J. Thumrongvut, J. Suebsuk, and S. Sookasem, "Flexural strength of notched concrete beam filled with alkali-activated binders under different types of alkali solutions," *Construction and Building Materials*, vol. 127, pp. 673–678, 2016.

[30] ACI 211.4R-93, *Guide for Selecting Proportions for High-Strength Concrete with Portland Cement and Fly Ash*, American Concrete Institute, Farmington Hills, MI, USA, 1993.

[31] ACI 211.1-91, *Standard Practice for Selecting Proportions for Normal, Heavyweight, and Mass Concrete*, American Concrete Institute, Farmington Hills, MI, USA, 1991.

[32] D. Hardjito, S. E. Wallah, D. M. J. Sumajouw, and B. V. Rangan, "On the development of fly ash-based geopolymer concrete," *ACI Materials Journal*, vol. 101, no. 6, pp. 467–472, 2004.

[33] ASTM C143/C143M-15a, "Standard test method for slump of hydraulic-cement concrete," *Annual Book of ASTM Standard*, ASTM International, West Conshohocken, PA, USA, 2015.

[34] ASTM C403/C403M-16, "Standard test method for time of setting of concrete mixtures by penetration resistance," in *Annual Book of ASTM Standard*ASTM International, West Conshohocken, PA, USA, 2016.

[35] ASTM C469, "Standard test method for static modulus of elasticity and Poisson's ratio of concrete in compression," in *Annual Book of ASTM Standard*ASTM International, West Conshohocken, PA, USA, 2002.

[36] ASTM C78, "Standard test method for flexural strength of concrete (using simple beam with third-point loading)," in *Annual Book of ASTM Standard*ASTM International, West Conshohocken, PA, USA, 2002.

[37] A. Sathonsaowaphak, P. Chindaprasirt, and K. Pimraksa, "Workability and strength of lignite bottom ash geopolymer mortar," *Journal of Hazardous Materials*, vol. 168, no. 1, pp. 44–50, 2009.

[38] T. Sinsiri, T. Phoo-ngernkham, V. Sata, and P. Chindaprasirt, "The effects of replacement fly ash with diatomite in geopolymer mortar," *Computers and Concrete*, vol. 9, no. 6, pp. 427–437, 2012.

[39] S. Hanjitsuwan, S. Hunpratub, P. Thongbai, S. Maensiri, V. Sata, and P. Chindaprasirt, "Effects of NaOH concentrations on physical and electrical properties of high calcium fly ash geopolymer paste," *Cement and Concrete Composites*, vol. 45, pp. 9–14, 2014.

[40] U. Rattanasak and P. Chindaprasirt, "Influence of NaOH solution on the synthesis of fly ash geopolymer," *Minerals Engineering*, vol. 22, no. 12, pp. 1073–1078, 2009.

[41] A. Hawa, D. Tonnayopas, W. Prachasaree, and P. Taneerananon, "Development and performance evaluation of very high early strength geopolymer for rapid road repair," *Advances in Materials Science and Engineering*, vol. 2013, Article ID 764180, 9 pages, 2013.

[42] F. Pacheco-Torgal, J. P. Castro-Gomes, and S. Jalali, "Adhesion characterization of tungsten mine waste geopolymeric binder. Influence of OPC concrete substrate surface treatment," *Construction and Building Materials*, vol. 22, no. 3, pp. 154–161, 2008.

[43] F. Pacheco-Torgal, J. A. Labrincha, C. Leonelli, A. Palomo, and P. Chindaprasirt, *Handbook of Alkali-Activated Cements, Mortars and Concretes*, WoodHead Publishing Limited-Elsevier Science and Technology, Cambridge, UK, 2014.

[44] P. Chindaprasirt, T. Chareerat, S. Hatanaka, and T. Cao, "High strength geopolymer using fine high calcium fly ash," *Journal of Materials in Civil Engineering*, vol. 23, no. 3, pp. 264–270, 2011.

[45] C. Ridtirud, P. Chindaprasirt, and K. Pimraksa, "Factors affecting the shrinkage of fly ash geopolymers," *International Journal of Minerals, Metallurgy, and Materials*, vol. 18, no. 1, pp. 100–104, 2011.

[46] K. Sagoe-Crentsil, T. Brown, and A. Taylor, "Drying shrinkage and creep performance of geopolymer concrete," *Journal of Sustainable Cement-Based Materials*, vol. 2, no. 1, pp. 35–42, 2013.

[47] S. Songpiriyakij, T. Pulngern, P. Pungpremtrakul, and C. Jaturapitakkul, "Anchorage of steel bars in concrete by geopolymer paste," *Materials & Design*, vol. 32, no. 5, pp. 3021–3028, 2011.

[48] P. K. Sarker, "Bond strength of reinforcing steel embedded in fly ash-based geopolymer concrete," *Materials and Structures*, vol. 44, no. 5, pp. 1021–1030, 2011.

[49] P. K. Sarker, S. Kelly, and Z. Yao, "Effect of fire exposure on cracking, spalling and residual strength of fly ash geopolymer concrete," *Materials & Design*, vol. 63, pp. 584–592, 2014.

[50] M. Sofi, J. S. J. van Deventer, P. A. Mendis, and G. C. Lukey, "Engineering properties of inorganic polymer concretes (IPCs)," *Cement and Concrete Research*, vol. 37, no. 2, pp. 251–257, 2007.

[51] P. Nath and P. K. Sarker, "Flexural strength and elastic modulus of ambient-cured blended low-calcium fly ash

geopolymer concrete," *Construction and Building Materials*, vol. 130, pp. 22–31, 2017.

[52] M. Shariq, J. Prasad, and H. Abbas, "Effect of GGBFS on age dependent static modulus of elasticity of concrete," *Construction and Building Materials*, vol. 41, pp. 411–418, 2013.